GAVIN PUBLISHERS

Journal of Pharmacovigilance and Pharmacotherapeutics

Research Article

Baki VB, et al. J Pharmacovigil Pharm Ther: JPPT-125.
DOI: 10.29011/JPPT-125. 100025

Homology Modeling, Docking and Structure Based Virtual Screening Against AcrB Efflux Pump of Multidrug Resistant *Salmonella*

Vijaya Bhaskar Baki[1], Muni Chandra Babu Tirumalsetty[1], Vijaya Kumar Bathala[2], Rajendra Wudayagiri[1*]

[1]Division of Bioinformatics, Department of Zoology, Sri Venkateswara University, Tirupati, A.P, India

[2]Department of Biotechnology, Sri Venkateswara University, Tirupati, A.P, India

[*]**Corresponding author:** Rajendra Wudayagiri, Department of Zoology, Sri Venkateswara University, Titurpati-517502, India. Tel: +919849667236; Email: rajendraw2k@yahoo.co.in ; vijaybio08@gmail.com

Citation: Baki VB, Tirumalsetty MCB, Bathala VK, Wudayagiri R (2018) Homology Modeling, Docking and Structure Based Virtual Screening Against AcrB Efflux Pump of Multidrug Resistant *Salmonella*. J Pharmacovigil Pharm Ther: JPPT-125. DOI: 10.29011/JPPT-125. 100025

Received Date: 20 December, 2017; **Accepted Date:** 11 January, 2018; **Published Date:** 17 January, 2018

Abstract

AcrB efflux pump is an inner transmembrane protein that belong to the RND transporters family. AcrB plays an important role in the extrusion of diverse structural compounds from the cytoplasm and periplasmic region to the exterior of the gram negative bacterial cell and considered as potential drug target for the discovery of efflux pump inhibitors (EPIs). In the present study, we constructed AcrB model based on the crystal structure of AcrB from *E. coli* (PDBID: 2j8s). Structural analysis revealed that AcrB is mainly composed of three structural domains such as transmembrane (TM) domain, pore domain and docking domain. TM domain consists of 12 TM helices which traverse the inner lipid bi layer. Pore domain is present in the periplasm region and contains four subdomains viz., PN1, PN2, PC1 and PC2, and formed distal and proximal binding pockets. Molecular docking study documented that tetracycline, cefsulodin, penicillin, ceftazamid, lincomycin, chloramphenicol, meropenum and aminoglycoside have shown significant interactions with distal pocket whereas carbenicillin has explicated towards proximal pocket. Moreover, virtual screening using ZINC and PubChem database against AcrB that enlighten ten potent lead molecules: ZINC28475998 (-11.2), ZINC28476198 (-11.1), ZINC28477171 (-10.9), ZINC28475792 (-10.6), ZINC27182211 (-9.2), CID11143966 (-9.6), CID44265715 (-9.5), CID102503 (-9.1), CID11902980 (-9.0) and CID22845248 (-9.0) with greater binding affinities and displayed marked interactions with decisive residues of proximal and distal binding pockets. Accordingly, these lead molecules could be helpful for the development of efflux pump inhibitors and might restore the conventional antibiotics longer time within the bacteria.

Keywords: AcrB Efflux Pump; Antibiotics; Homology Modeling; PaβN; Virtual Screening

Introduction

Salmonella enterica serovar Typhimurium is gram negative bacteria and belongs to the *Enterococci* sps which causes serious health problems such as gastroenteritis, bacteremia and typhoid fever. Multidrug resistance *Salmonella* out breaks had been found in United States [1,2] United Kingdom [3,4] in poultry, beef and swine [5-8]. Prevalence of multidrug resistance to numerous antibiotics reported to occur due to gene mutation in target protein, target modification, drug inactivation, target bypassing, horizontal gene transfers and dysfunction of efflux pumps [9,10]. Efflux pumps are majorly associated with resistance of both gram negative and gram positive bacteria and categorized into five types such as ATP binding cassette (ABC), Resistance Nodulation Division family (RND), Major Facilitator Super family (MFS), Small Multidrug Resistance (SMR) protein family (SMR) and Multidrug and Toxic Compound Extrusion (MATE). Among RND transporters are highly expressed in several gram-negative bacteria such as *E. coli, Pseudomonas aeruginosa, Klebsiella pneumonia, Acinetobacter baumanni* and *Enterococcus* sps [11]. However, Complete genome sequencing of *Salmonella* has shown the existence of nine efflux pumps that belongs to the various transporter family such as ABC (macAB), RND (AcrAB, AcrCD, AcrEF, mdsABC, mdsABC), MFS (EmrAB, mdgA) and MATE (mdtk) [12,13]. RND efflux

pump play an important role especially in gram negative bacterial pathogens and to show broad spectrum substrate specificity to a wide array of diverse compounds such as dyes (acriflavin and ethidium), antibiotics (macrolides, fluoroquinolones, β-lactams, tetracycins, chloramphenicol, rifampin, novobiocin, fusidic acid), detergents (bile salts, tritonX-100, SDS) and some organic solvents (hexane, heptanes, octane and nonane or cyclohexane) [14,15]. RND transporter is huge complex that composed with three proteins such as inner transmembrane protein, periplasmic adaptor protein and outer transmembrane protein and it traverse both inner and outer membrane lipid bilayer. Inner transmembrane protein has several binding pockets which allow the binding of numerous diverse compounds by obtaining the energy from the proton translocation motive force, this phenomenon is highly conserved in bacteria. The fabulous function of RND pump clearly indicates that its acts as attractive broad spectrum molecular target for designing of novel efflux pump inhibitors. RND efflux pump may be thwarted in several ways such as altering the regulatory mechanism, inhibiting the functional assembly of multicomponent proteins, inhibiting the proton translocation mechanism, blocking the outer membrane protein, the functional group modification of existing drugs and altered sensitivity to the competitive and non-competitive inhibitors. So far, a little number of Efflux Pump Inhibitors (EPIs) have been discovered to deny the efflux pump activity such as globomycin by blocking of functional assembly of tripartite complex, carbonyl cyanide m-chlorophenyl hydrazone (cccp) and potassium cyanide which collapse the proton motive force of the pump and PAβN itself is a substrate of efflux pumps and act as competitive inhibitor. Generally, PAβN is used as EPI to treat gram negative bacteria and restore the activity of various antibiotics (chloramphenicol, macrolide, oxazolidinones and rifampicin). Keeping in view, the present study is undertaken to explicate the binding properties of various antibiotics and the novel potent EPIs for clinical management of gram negative bacterial infections.

Materials and Methods

Prediction of Secondary Structure and TM α-helices

Protein sequence of AcrB (Acc No: Q8ZRA7) was retrieved from SWISSPROT and Physicochemical properties such as Aliphatic index, Grand average of hydropathy (GRAVY) and Theoretical pI value were calculated using Protparam Secondary structural elements such as alpha helix, extended sheets, beta turns and random coils were predicted using different servers Viz., SOPMA [16], GOR4 [17] and Chou & Fosman. TM α-helices were predicted using different servers such as TMHMM [18], TMpred [19], SOSUI [20] and HMMTOP [21] to confirm origin and end of the helices.

Protein Modeling and Validation

Initially, template structure was selected by performing BLASTp search against Brookhaven Protein Data Bank (PDB) on the basis of sequence identity with high score, less e-value, highest resolution and R-factor. Ensuing, the coordinates for the query structure were assigned from template structure by means of pairwise sequence alignment using ClustalX [22]. Subsequently, 3D structures of AcrB were built by using MODELLER 9.14 [23]. Ensuing, the model has lowest DOPE Score was taken and amended irregular secondary structures such as α-helices, β-strands and superfluous loops by adopting MODLOOP Server [24]. Then, model was energy minimized by applying the force field of GROMOS96 using SPDBV software. The quality of the model was corroborated by calculating the stereo chemical properties, compatibility of the atomic model (3D) with its own amino acid resides (1D), bond lengths, bond angles and side chain planarity using SAVES server. Ramachandran plot calculations to check the stereo chemical quality of protein structure using PROCHECK [25] Environment profile using Verify3D [26] and ERRAT [27]. The residue packing and atomic contact were analyzed using WHATIF and Z Score of Ramachandran plot was calculated using WHATCHECK [28] Root Mean Square Deviation (RMSD) was calculated by superimposition of 3D-Model with template using SPDBV [29]. This final refined model was used for docking studies.

Retrieval of Ligands

Antibiotics such as tetracycline, penicillin, chloramphenicol, aminoglycoside, meropenem, cefsulodin, carbepenem, lincomycin, and ceftazamide, efflux pump inhibitor (PaβN) and its analogues were downloaded from PubChem (http://www.ncbi.nlm.nih.gov/pccompound) and ZINC database (https://docking.org/).

Structure Based Virtual Screening and Docking

Molecular docking simulations and virtual screening was carried out by using AUTODOCK VINA 4.0 [30] with PyRx [31] interface tool. Initially, energy of all the ligands were minimized by applying the Universal Force Field (UFF) using conjugate-gradient algorithm with 200 run iterations and converted into PDBQT format. Subsequently, virtual screening was employed by using Lamarckian genetic algorithm and parameters were set with 150 Number of individual population, 25000 Max number of energy evaluation, 27000 Max number of generation, one among the top individuals to survive to the next generation, Gene mutation rate of 0.02, Crossover rate of 0.8, Cauchy beta of 1.0 and GA window size of 10.0. The grid was set to pore region of efflux pump at X=29.3901, Y= -42.745, Z= -51.82 and dimensions (Å) at X= 90.000, Y= 105.7097, Z= 104.2448 with exhaustiveness 8. The best docked ligand conformations were sorted out and scrutinized the bond angle, lengths and, binding interactions using PyMol [32].

Results and Discussion

Assessment of Primary, Secondary and TM α-helices

Analysis of physico-chemical properties was found to be aliphatic index (105.02), grand average of hydropath city (0.273), theoretical PI (5.47), extinction coefficients (8.0345) and the instability index (31.13). Secondary structure analysis has shown 76.1% alpha helix with 789 residues using the method of Chou & Fasman, 44.74% with 464 residues using SOPMA, 42.62% with 442 residues using GOR4. Extended strands showed 55.2% with 572 residues by Chou & Fasman, 19.77% with 205 residues by SOPMA and 15.14% with 157 residues by GOR4. Random coil confers 42.24% with 438 residues by GOR4, 27.39% with 284 residues and 9.6% with 100 residues by Chou & Fasman. Beta turn exhibits 5.2% with residues 84 by SOPMA and GOR4 whereas Chou & Fasmon was failed to provide beta turns (Figure 1). Twelve TM α-helices were predicted and shown in Table 1. Helix-I is started at residues position 9 and end at the 111 residues portion. Helix-II (158-432), Helix-III (366-459), Helix-IV (392-489), Helix-V (438-543), Helix-VI (470-580), Helix-VII (541-639), Helix-VIII (688-966), Helix-IX (898-977), Helix-X (925-1081), Helix-XI (974-1068) and Helix-XII (1006-1101). Besides, Helix-XIII (1088-1109) was identified by TMpred while HMMTOP, SOUSI and TMHMM were failed to found Helix- XIII and SOUSI also failed to predict Helix10.

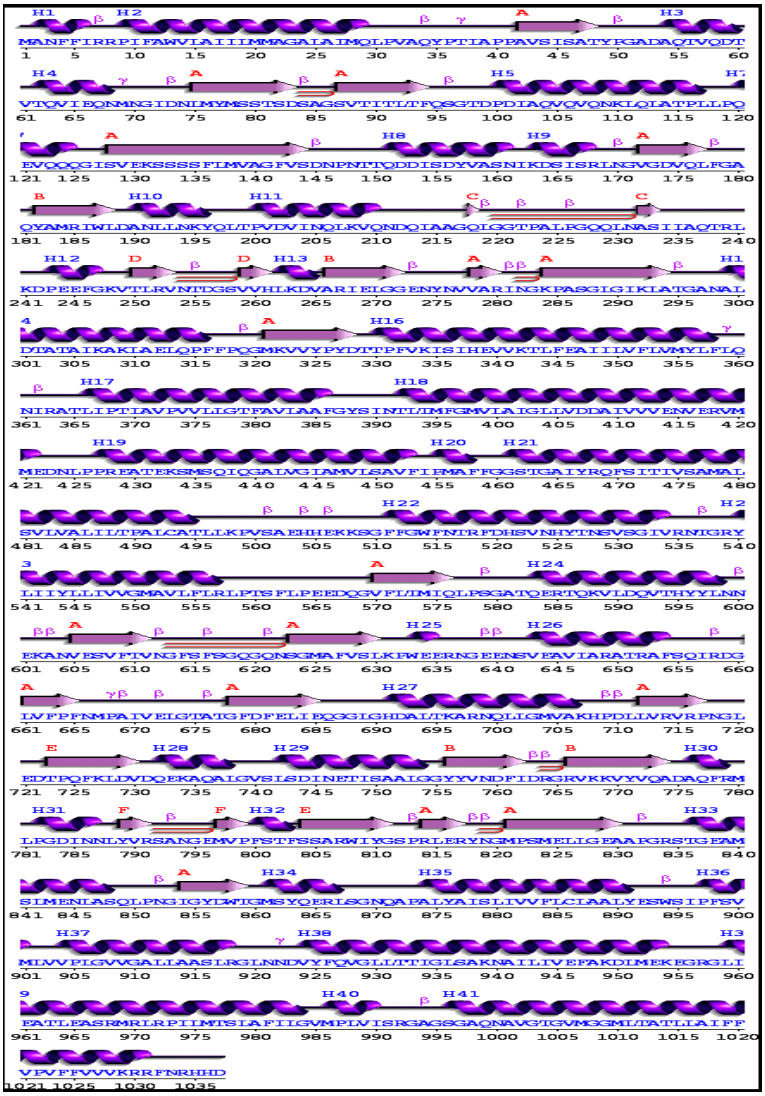

Figure 1: Secondary Structure of AcrB efflux pump of *Salmonella*.

TM Helix	HMMTOP		SOSUI		TMHMM		TMPred	
	Start	End	Start	End	Start	End	Start	End
Helix1	82	101	83	105	9	31	92	111
Helix2	413	432	408	430	337	359	158	177
Helix3	439	458	437	459	366	388	427	445
Helix4	467	486	467	489	392	414	453	473
Helix5	515	534	514	536	438	460	521	543
Helix6	547	570	549	571	470	492	553	580
Helix7	614	631	613	635	541	563	623	639
Helix8	945	964	944	966	872	891	688	713
Helix9	971	990	969	991	898	920	959	977
Helix10	1001	1018	-	-	925	947	979	1000
Helix11	1047	1064	1046	1068	974	996	1007	1028
Helix12	1077	1101	1079	1101	1006	1028	1056	1077
Helix13	-	-	-	-	-	-	1088	1109

Table 1: Prediction of TM helices by using different servers.

Protein Modeling and Validation

As results of BLASTp showed nine proteins such as 1IWG, 1OY6, 2J8S, 2GIF, 3NOC, 2HQG, 1T9T, 2HQD from *E. coli* and 2V50 from *Pseudomonas aeruginosa* which have highest identity of 97%, query coverage of 98% and low e-value. Despite all proteins showed highest identity with AcrB, 2J8S was selected as template due to lowest resolution of 2.5Å and R–factor 0.22. Sequence alignment was carried out between template and query sequence, and hundred models were generated using MODELLER 9.14 (Figure 2). The assessment of final model demonstrated that stereo chemical property was elucidated using PROCHECK that Ramachandran plot exhibited that 94.5% with 856 residues were aligned within the most favored regions (A, B, L), 5.1% with 46 residues were located within additional allowed region, 0.2% with 2 residues were located within generously allowed region, no residues were aligned within disallowed region (Figure 3A). WHATCHECK program showed Z-score of 1.193 for the 2nd generation packing quality, 0.386 for the Ramachandran plot appearance and 0.347 for the chi1/chi2 rotamer normality. The bond length, bond angles, omega angle restraints, planarity of side chain, improper dihedral distribution and inside/outside distribution were found to be 0.98, 1.175, 0.625, 0.277, 0.866 and 1.066. The overall quality factor of 90.12% was observed by using ERRAT environment profile (Figure 3B). Verify3D showed that 67.8% residues had an average 3D-1D score above 2 indicated that the model was highly reliable **(**Figure 3C).

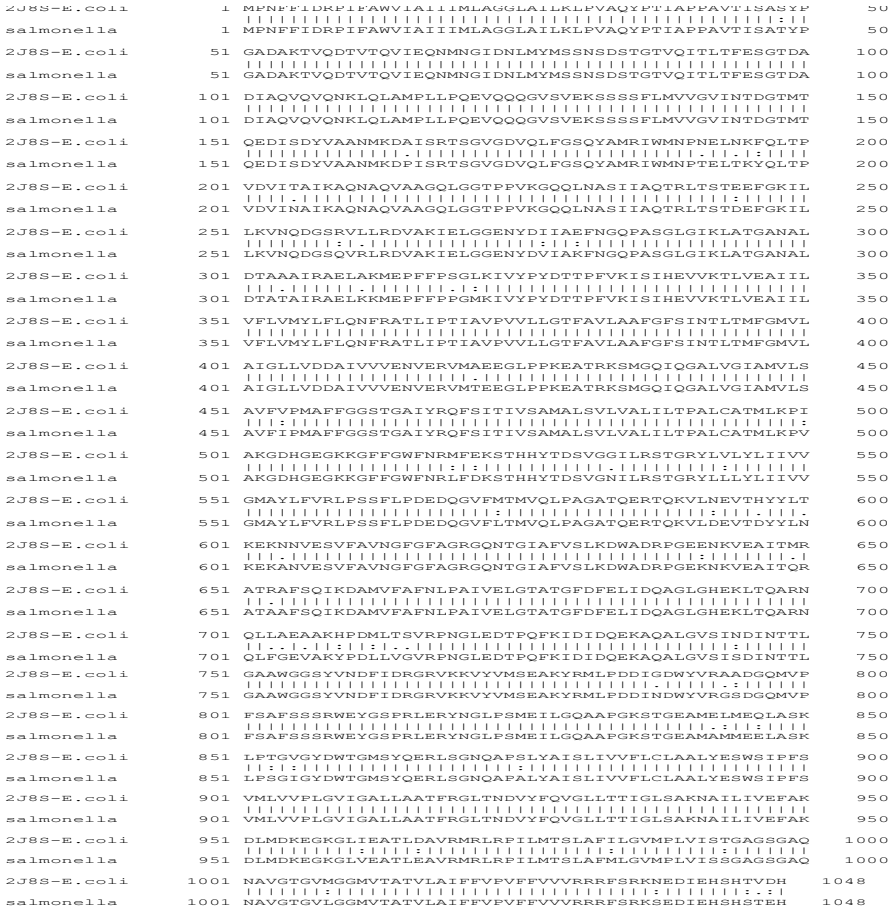

Figure 2: Pair wise sequence alignment of AcrB efflux pump of *Salmonella* with AcrB efflux pump of *E. coli.*

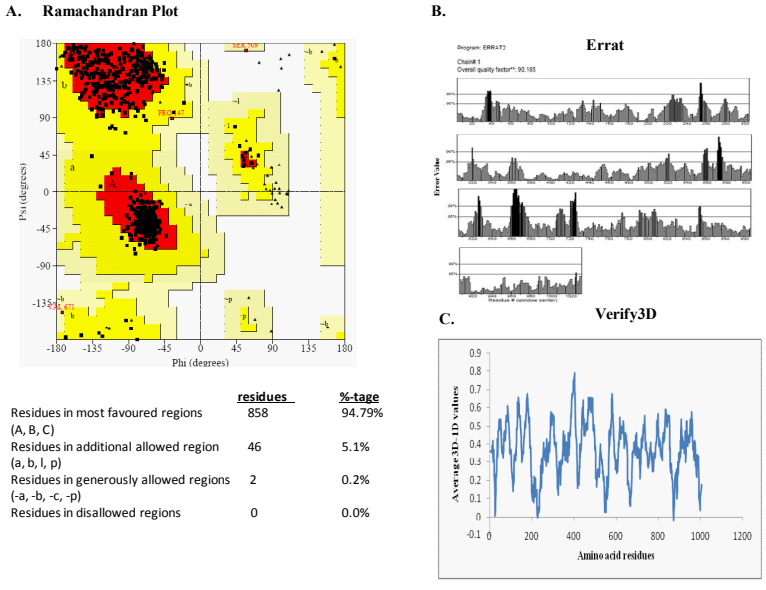

	residues	%-tage
Residues in most favoured regions (A, B, C)	858	94.79%
Residues in additional allowed region (a, b, l, p)	46	5.1%
Residues in generously allowed regions (-a, -b, -c, -p)	2	0.2%
Residues in disallowed regions	0	0.0%

Figures 3(A-C): A). Ramachandran plot, **B**). Statistics of non-bonded interactions of AcrB efflux pump was calculated by ERRAT, **C**). 3D model compatibility of AcrB efflux pump was adopted by using Verify 3D.

Architecture of AcrB Efflux Pump

AcrB pump is composed of three major domains such as TM domain, pore domain and docking domain (Figure 4a). TM domain contains twelve TM α-helices, six TM α-helices such as Helix-I, Helix-II, Helix-III, Helix-IV, Helix-V and Helix-VI are arranged as symmetrically at N-terminal to six TM α-helices such as Helix-VII, Helix-VIII, Helix-IX, Helix-X, Helix-XI and Helix-XII at C-terminal. TM α-helices traverse the inner lipid bilayer and exhibit a pseudo two-fold symmetry, and play an important role in the proton translocation across lipid bilayer that catalyzed by three conserved residues of Asn407 and Asp480 of TM Helix-IV and Lys940 of TM Helix-X (Figures 4b, 4c). Pore domain consists of four sub domains such as PN1, PN2, PC1 and PC2, PN1 and PN2 domains are formed with TM Helix-I and TM helix-II at N-terminal whereas PC1 and PC2 are formed with TM helix-VII and TM helix-VIII at C-terminal (Figure 4d). Moreover, each sub domain consists of two β-strands-α-helix-β-strand structural motif and sandwiched with each other. Docking domain composed of two sub domains such as DN and DC, each sub domain has four β-sheets in which two antiparallel β-strands are parallel to hair pin structure. In addition, a beak like long hairpin loop structure (Gln210-Pro243) protrudes from DN and a vertical hairpin that composed of two small beta sheets linked to second motif of PN2 by short connecting loop (Gly272-Val278). DC domain is extended from the first motif of PC2 sub domain through the connecting loop (Val730-Gln732) and has vertical hairpin which linked to second motif of PC2 by connecting loop (Gly811-Arg814).

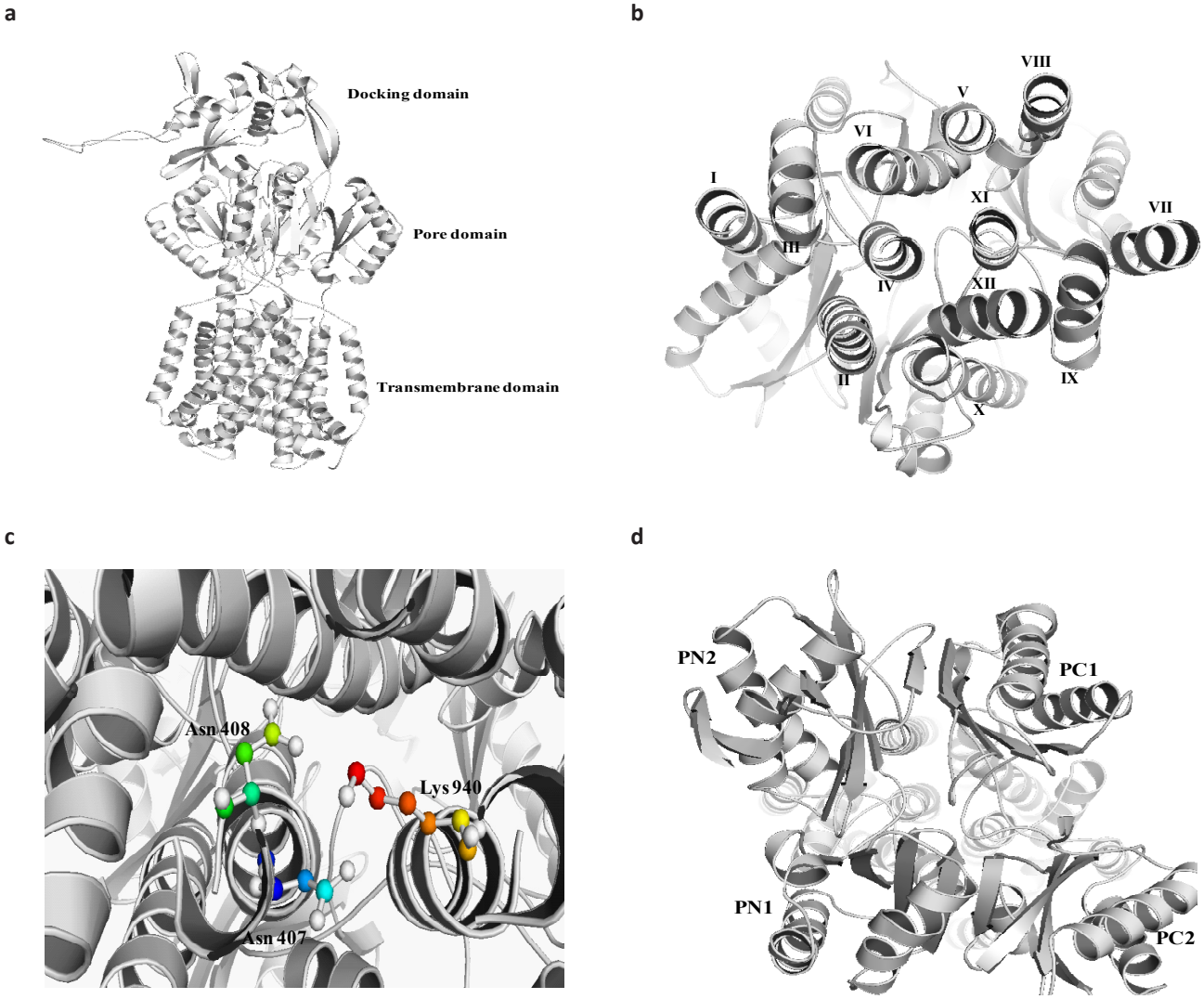

Figures 4(a-d): a). AcrB efflux pump with three domains such as transmembrane domain, periplasmic domain and docking domain, **b.)** Twelve transmembrane helices, **c.)** Proton translocation is catalysed by conserved residues of Asn407 and Asp408 of TM HelixIV, and Lys940 of Helix-X

(Residues are represented in green colour), **d.)** Pore domain consists of four subdomains such as PN1, PN2, PC1 and PC2.

Docking Simulation of Antibiotics

Docking simulation results showed that tetracycline, cefsulodin, penicillin, carbenicilin, ceftazamide, lincomycin, aminoglycosides, meropenem and chloramphenicol have shown interaction with distal pocket whereas carbenicilin has shown interactions with proximal pocket (Figure 5a: Table 2). Tetracycline has exhibited highest binding energy of -8.9 kcal/mol and formed nine interactions such as two bonds with OH group of Thr48, two bonds with Gly51, two bonds with Ala85 and Ala273, three bonds with polar amide of Asn274 and Gln619. Cefsulodin displayed nine interactions Viz., three bonds with OH of Thr49, Ser46 and Ser87, five bonds with polar amide of Asn274, Gln176 and Gln619, one bond with Ala85 and showed binding energy of -8.4 kcal/mol. Penicillin displayed four interactions, two bonds with polar amide of Gln34, OH group of Thr34 and two bonds with Ile39 and Ala39, and conferred binding affinity of -8.3 kcal/mol. Ceftazidime has shown binding energy of -8.2 kcal/mol and explicated six bonds such as five bonds with OH group of Ser44, Thr89 and Thr91, polar amide of Gln176 and, aromatic ring of Phe616. Lincomycin showed binding energy of -7.6 kcal/mol and formed three bonds such as one bond with polar amide of Gln619, one bond with amino group of Lys769 and one bond with OH of Tyr771. Aminoglycoside showed binding energy of -7.2 kcal/mol and exhibited four binding interactions, two bonds with OH of Thr48 and two bonds with polar amide of Gln125. Meropenem has shown binding energy of -7.0 kcal/mol and conferred four bonds, two interactions with polar amide of Gln125 and Asn274, two bonds with OH of Thr771. Chloramphenicol showed lowest binding energy of -6.8 kcal/mol and formed five bonds, one bond with OH of Thr48, two bonds with amino group of Arg185, one bond with COO^- of Glu273 and one bond with Gly754. Carbenicillin has affinity of -8.2 kacl/mol for proximal pocket and displayed two bonds viz., one bond with COO^- of Gln576 and Gly719. PAβN is efflux pump inhibitor that bound in close proximity to proximal pocket with binding energy of -8.7 kcal/mol and formed interactions with OH group of Tyr467 and Thr560, polar amide of Asn922 and Gln927 (Figure 5b).

a Tetracycline

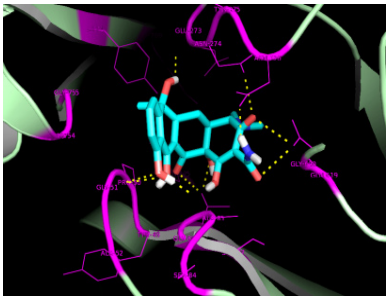

Cefsulodin

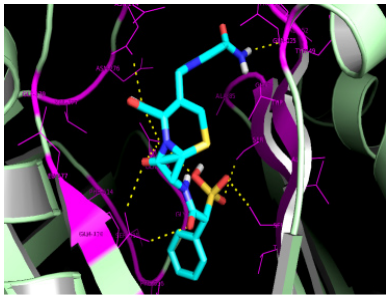

Penicillin

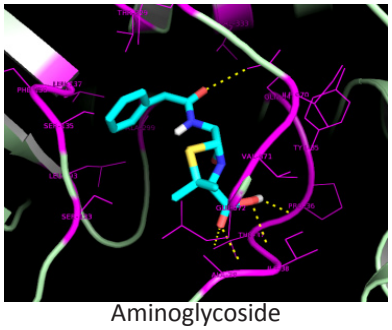

Ceftazamide

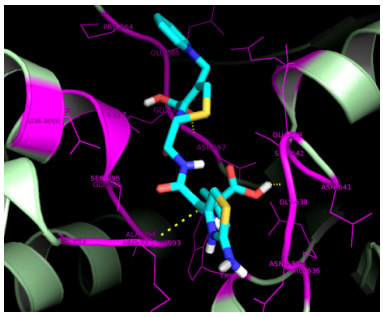

Lincomycin

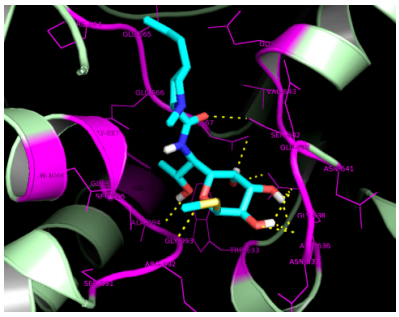

Aminoglycoside

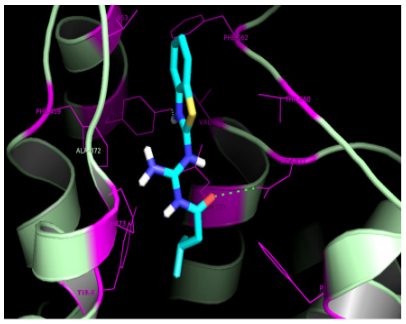

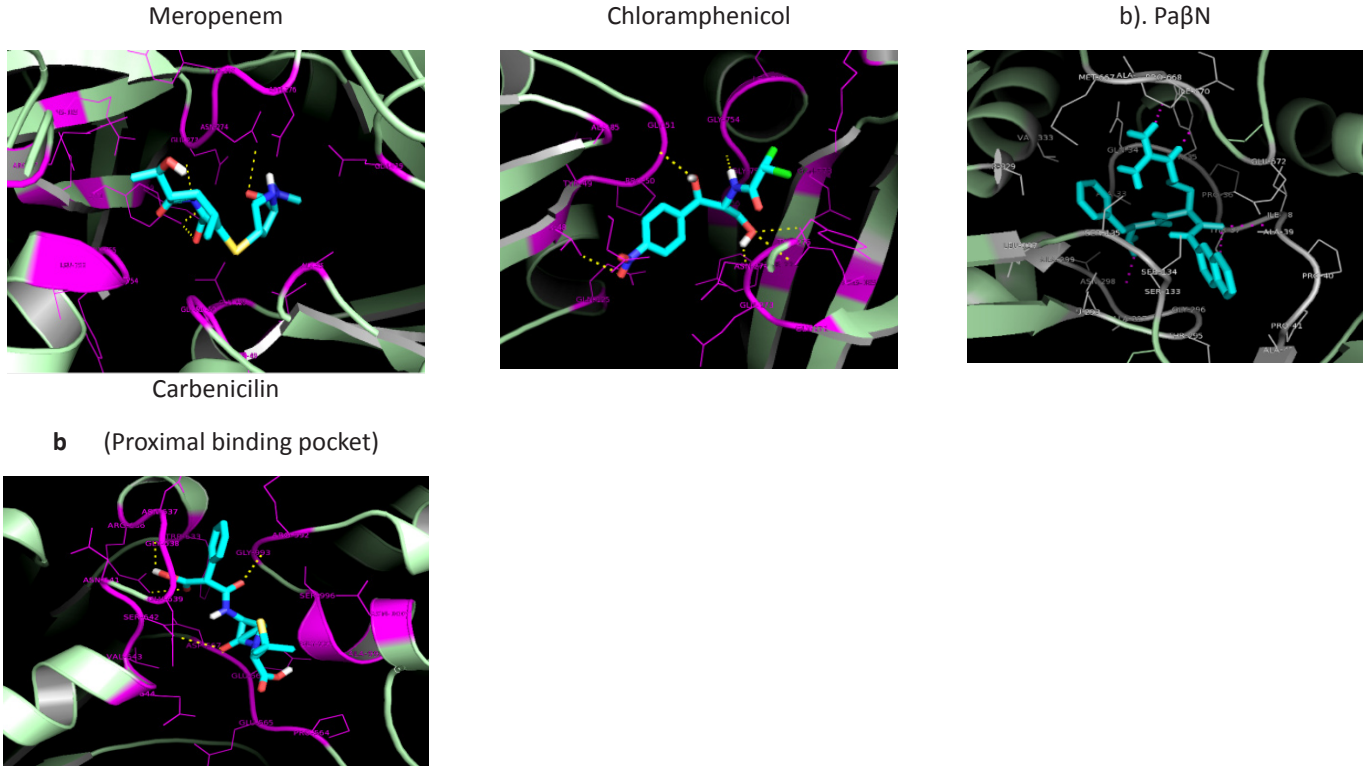

Figures 5(a-b): a). Binding pose of antibiotics and b). PAβN within the distal and proximal pocket of periplasmic domain of AcrB efflux pump.

Antibiotics	Structure	Binding Interaction	Distance (Å)	Binding energy Kcal/mol ΔG
Tetracycline	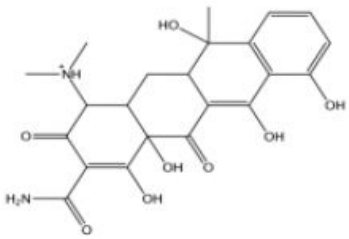	29HO-----Thr48 38HO-----Thr48 34HO-----Gly51 36HO-----Gly51 26HO-----la85 23HO-----Ala273 30HO-----Asn274 28HO-----Gln619 30HO-----Gln619	3.3 2.7 3.0 3.3 2.2 2.1 3.2 3.1 3.1	-8.9
Cefsulodin	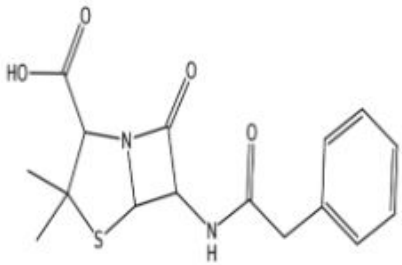	17OC-----Thr49 39OC-----Ser46 17OC-----Ala85 38OC-----Ser87 32OC-----Gln176 41OC-----sn274 21OC-----Gln619 31OC-----Gln619 34OC-----Gln619	2.4 2.9 2.8 3.3 3.0 3.0 3.1 3.1 3.4	-8.4

Penicilin	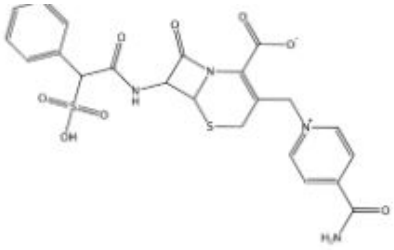	22OC-----Gln34 14HO-----Thr37 22OC-----Ile38 15HO-----Ala39	3.1 2.3 3.5 3.0	-8.3
Ceftazidime	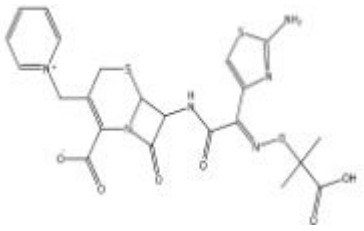	33OC-----Ser44 33OC-----Thr91 32OC-----Thr89 42OC-----Gln176 23OC-----Ser615 34OC-----Phe616	3.0 2.1 1.9 2.4 3.0	-8.2
Lincomycin	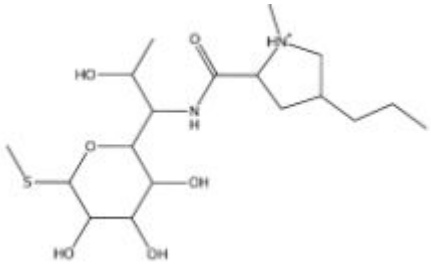	32OH-----Gln619 30OH-----Lys769 30OH-----Tyr771	3.2 3.5 2.8	-7.6
Aminoglycoside	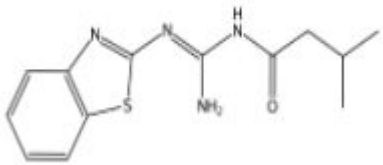	18HO-----Thr48 22HO-----Thr48 14HO-----Gln125 18HO-----Gln125	2.3 2.8 2.6 2.6	-7.2
Meropenem	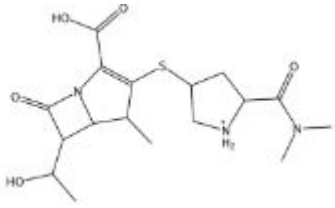	17HN-----Gln125 22HO-----Asn274 28HO-----Tyr771 29HO-----Tyr771	3.5 2.9 3.0 3.1	-7.0
Chloramphenicol	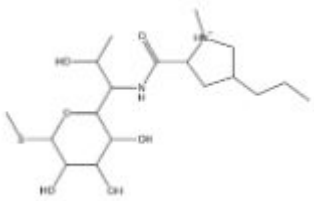	17ON-----Thr48 14HO-----Pro50 16HO-----Arg185 16HO-----Arg185 23OH-----Glu273 22HN-----Gly754	2.9 3.2 2.9 3.2 2.1 2.3	-6.8

Carbenicillin	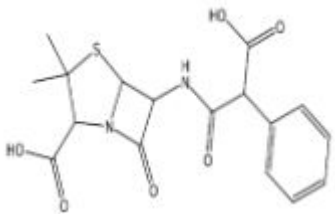	24OH-----Ser642 34OC-----Gly993 19OC-----Arg636 25OH-----Gly638	3.2 1.9 1.4 2.9	-8.2
PAβN	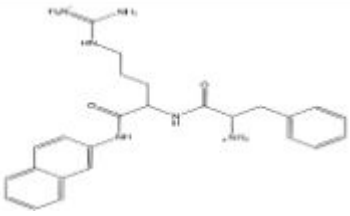	43HN-----Thr560 40HN-----yr467 40HN-----Gln927 33OC-----Asn922	2.3 2.4 2.2 3.1	-8.7

Table 2: H-bonds, distance and binding affinities of antibiotics with active site residues of AcrB efflux pump.

Virtual Screening and Docking

In order to explicate the selective EPIs, virtual screening was performed using ZINC and PubChem database against AcrB efflux pump and performed docking simulation that revealed ten best lead compounds with different scaffolds (Figure 6: Table 3). Nine compounds have shown best binding affinity for proximal pocket whereas ZINC28477171 has shown significant binding affinity to distal pocket. ZINC28475998 and ZINC28476198 compounds exert highest binding affinities of -11.2 and -11.1 kcal/mol. ZINC28475998 formed three H-bonds such as 30NH, 32NH and 29NH groups with COO^- of Glu682 and Glu825, OH of Ser823 and one arene-arene interaction between napthalene and benzene of Phe616. ZINC28476198 formed six interactions such as 23HN, 32HN, 30HN and 30HN with OH of Ser79 and Ser823, COO^- of Glu682 and Glu825, 48OC and 29OC with OH of Thr91 and COO^- of Glu864. ZINC28475792 has binding energy of -10.6 kcal/mol and formed five interactions viz., 32HN, 30HN, 34HN and 24HN with COO^- of Glu682, Arg817, COO^- of Glu825, COO^- of Glu825 and two hydrophobic interactions with Phe616 and Phe665. ZINC27182211 has shown binding energy of -9.2 Kcal/mol and formed two bonds, OH49 formed one bond with NH2 of Arg714 and NH42 formed one bond with polar amide of Asn718, and two arene-arene interactions with Phe616 and Phe665. CID11143966 exhibited binding energy of -9.6 kcal/mol and displayed hydrophobic interactions with Phe616, Phe665 and Phe663. CID44265715 and CID102503 have shown binding affinities of -9.2 kcal/mol and -9.1 kcal/mol, CID44265715 displayed five interactions, 29HN, 30HN, 30HN, 29HN and 26HN groups formed bonds with COO^- of Gln576, OH of Ser615 and Ser617, polar amide of Asn718 and CID102503 formed six bonds, 23HN, 25HN and 27HN formed three bonds with polar amide and OH of Gln576, Ser615, Ser617 and Asn718 and three arene-arene interactions with Phe616 and Phe663. CID11902980 and CID22845248 have shown similar binding energies of -9.0 kcal/mol, CID11902980 made one polar interaction with Leu661 and non-polar interactions with Phe665 and Phe616 and CID22845248 formed three interactions, 31HN and 29HN formed two bonds with Pro717 and Asn718. ZINC28477171 has shown binding affinity of -10.9kcal/mol for proximal pocket and displayed nine polar interactions such as 60O=C, 58O=C, 57O=C formed four bonds with OH of Ser44 and Thr91, 35HN, 25HN, 31HN and 33HN formed four bonds with COO^- of Glu130, Asp174 and Glu825, and one arene-arene interaction with Phe616.

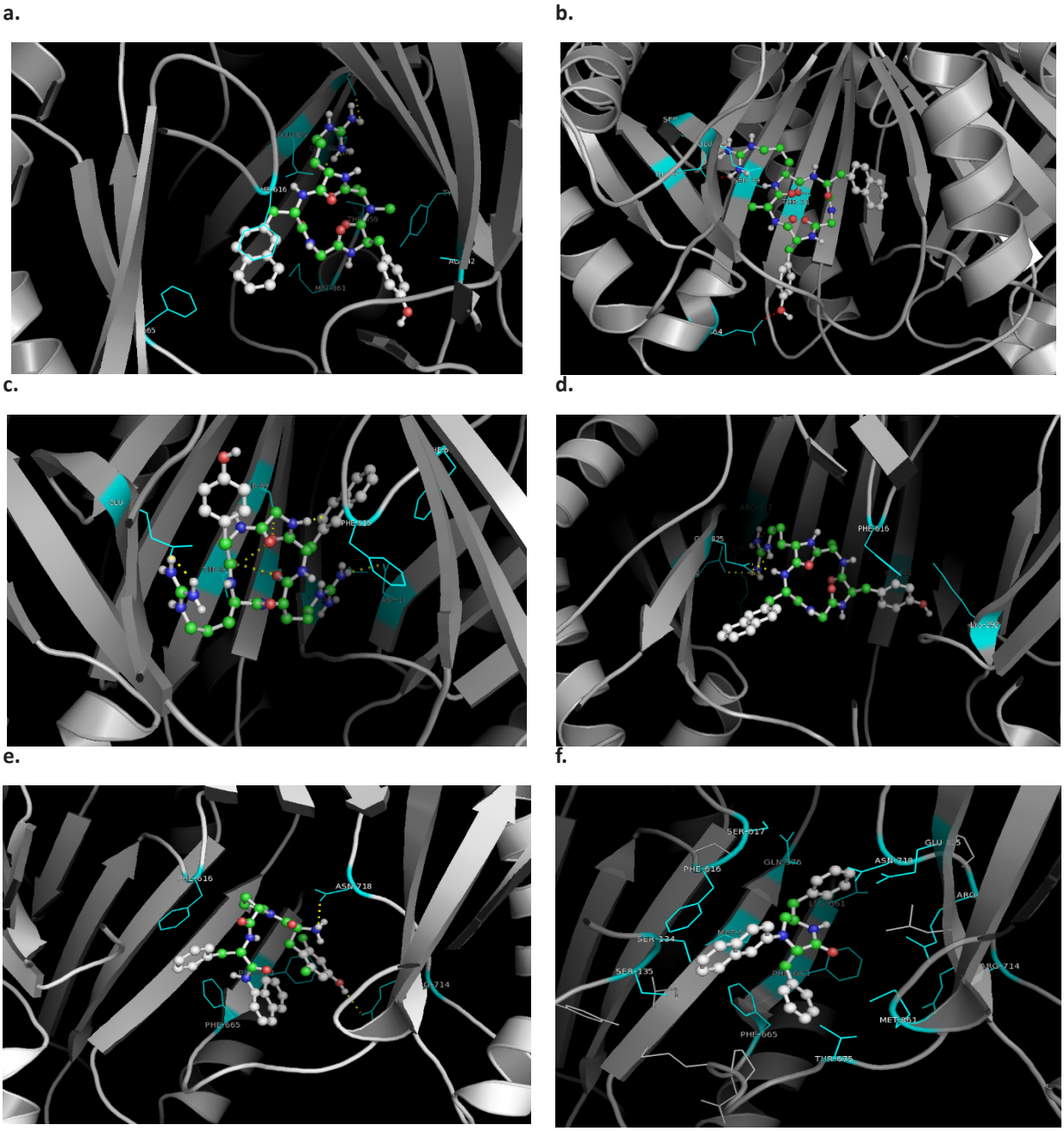

Figures 6(a-j): Binding pose of **a)**. ZINC28475998, **b)**. ZINC28476198, **c).** ZINC28477171, **d).** ZINC28475792, **e).** ZINC2718221, **f).** CID11143966, **g).** CID44265715, **h).** CID102503, **i).** CID11902980 and **j).** CID22845248 within the binding pocket of efflux pump.

ZINC Compound	Compound Name	Binding Interactions	Distance (∠)	Binding energy (kcal/mol ΔG)
ZINC28475998 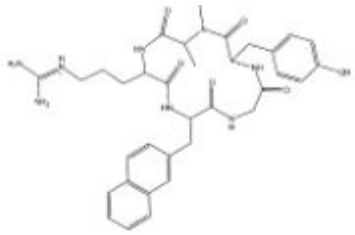	(2S)-1-[(2S)-2-amino-3-(4-hydroxy-2,6-dimethyl-phenyl) propanoyl]-N-[(1S)-1-benzyl-2-(1-naphthylamino	30HN-----Glu682 32HN-----Ser823 29HN-----Glu825	2.5 2.8 2.0	-11.2
ZINC28476198 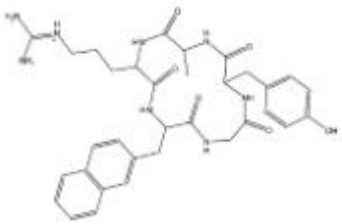	2-[3-[(2S,5S,11R,14R)-11-[(4-hydroxyphenyl)methyl]-14-methyl-5-(2-naphthylmethyl)-3,6,9,12,15-pentao	48OC-----Thr91 23HN-----Ser79 30HN-----Glu682 32HN-----Ser823 30HN-----Glu825 29OC-----Glu864	3.2 2.5 3.4 2.7 2.4 2.9	-11.1
ZINC28477171 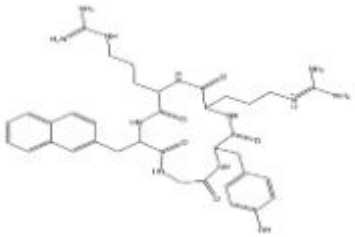	1-[3-[(2S,5S,11R,14R)-14-(3-guanidinopropyl)-11-[(4-hydroxyphenyl)methyl]-5-(2-naphthylmethyl)-3,6,9	60OC-----Ser44 58OC-----Thr91 57OC-----Thr91 60OC-----Thr91 35HN-----Glu130 35HN-----Asp174 25HN-----Phe616 31HN-----Glu825 33HN-----Glu825	2.7 2.6 3.1 2.7 2.2 2.7 1.9 3.3 2.3	-10.9
ZINC28475792 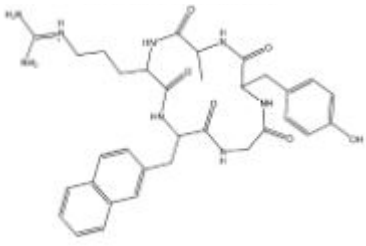	2-[3-[(2S,5S,11R,14S)-11-[(4-hydroxyphenyl)methyl]-14-methyl-5-(2-naphthylmethyl)-3,6,9,12,15-pentao	32HN-----Glu682 30HN-----Arg817 32HN-----Glu825 34HN-----Glu825 24HN-----Glu825	2.5 2.8 2.7 2.4 2.2	-10.6

ZINC27182211 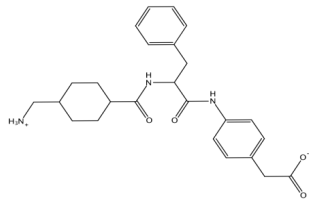	2-[3-[(2S,5S,11R,14S)-11-[(4-hydroxyphenyl) methyl]-13,14-dimethyl-5-(2-naphthylmethyl)-3,6,9,12,15-p	49HO-----Arg714 43HN-----Asn718	3.4 2.6	-9.2
CID11143966 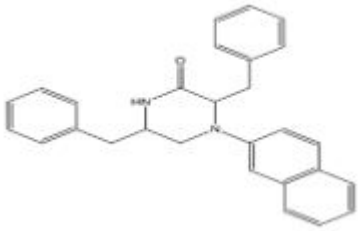	(3S,6R)-3,6-dibenzyl-4-naphthalen-2-ylpiperazin-2-one	Phe616, Phe665, Phe663, Leu661, Gln576, Ser134, Ser135	-	-9.6
CID44265715 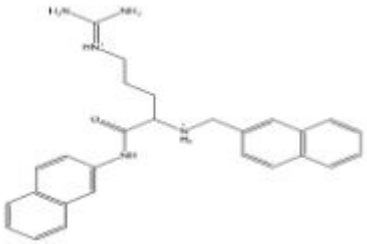	MK-56-(2S)-5-(diaminomethylideneamino)-N-naphthalen-2-yl-2-(naphthalen-2-ylmethylamino)pentanamide	29HN-----Gln576 30HN-----Gln576 30HN-----Ser615 29HN-----Ser617 26HN----------Asn718	2.0 2.7 2.4 2.7 2.0	-9.5
CID102503 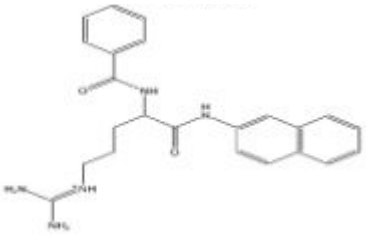	Nalpha-Benzoyl-DL-arginine-2-naphthylamide hydrochloride	23HN-----Gln576 25HN-----Gln576 23HN-----Ser615 23HN-----Ser617 27HN-----Asn718 27HN-----Asn718	2.5 2.6 2.7 2.7 2.2 2.7	-9.1
CID11902980 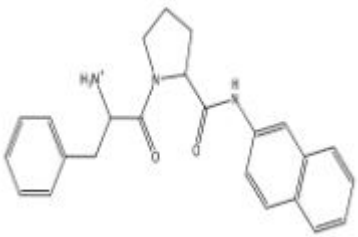	[(2S)-1-[(2S)-2-(naphthalen-2-ylcarbamoyl)pyrrolidin-1-yl]-1-oxo-3-phenylpropan-2-yl] azanium	29HN-----Leu661	2.5	-9.0

CID22845248 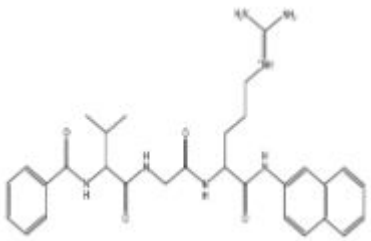	Nalpha-Benzoyl-DL-arginine-2-naphthylamide hydrochloride-BANA	31HN-----Pro717 29HN-----Asn718 29HN-----Asn718	2.4 2.4 2.0	-9.0

Table 3: H-bonds, distance and binding affinities of best lead compounds with active site residues of AcrB efflux pump.

Lipinski Rule of Five

Appraisal of pharmacological properties using Lipinski rule of five such as molecular weight, H-bond donors, H-bond acceptors and cLogP reveal that majority of the compounds are found to be satisfied as shown in Table 4. H-bond donors were predicted to be less than five and H-bond acceptors are less than ten. cLogP or partition coefficient plays a major role in accessing the drug in the body which was found to be less than five that indicates good absorption and distribution. Finally, most of the compounds obeyed Lipinski rule of five and could be help full in the development of EPIs for the inhibition of AcrB efflux pump.

Compound Name	Molecular weight	cLog	H-Don	H-Acc	TPSA	Rotatable bonds
ZINC28475998	659	0.33	10	14	223	8
ZINC28476198	645	0.21	11	14	229	9
ZINC28477171	368	2.9	1	5	55	5
ZINC28475792	645	0.21	11	14	229	9
ZINC27182211	579	3.8	6	8	125	9
CID11143966	406	6.4	1	2	32.3	5
CID44265715	439	3.9	4	3	106	9
CID102503	439	2.1	5	3	123	8
CID11902980	388	3.5	2	2	77	5
CID22845248	559	2.6	6	5	181	13

Table 4: Lipinski rule of five of best docked conformations.

Conclusion

Multidrug resistance in bacteria is most serious impairment to health care, currently no novel antibacterial agents are undertaken in clinical settings. In the present investigation, 3D structure of AcrB was constructed on account of unavailability and docking analysis observed that tetracycline, cefsulodin, penicillin, ceftazidime, lincomycin, aminoglycosides, meropenem and chloramphenicol confers significant interactions with distal binding pocket residues and carbenicillin was bound at proximal binding pocket. Virtual screening and docking revealed potent lead compounds such as ZINC28475998, ZINC27182211, ZINC28475792, ZINC28477171, ZINC28476198, CID22845248, CID11143966, CID44265715, CID11902980 and CID102503 with greater specificity and binding affinities en route for distal and proximal binding pockets. Consequently, these compounds have shown relevant drug likeness properties and could inhibit the efflux pump by competing with antibiotics and increase the residence time of antibiotics.

Acknowledgment

BVB is extending thanks to University Grant Commission, India for providing financial assistance in the form of RGNF. Authors are grateful to the Coordinator, Bioinformatics center, Department of Zoology, Sri Venkateswara University, Tirupati for providing bioinformatics facilities.

Conflict of Interest

All the authors declared that there is no conflict of interest.

References

1. Grein T, Flanagan DO, McCarthy T (1999) An outbreak of multidrug-resistant *Salmonella typhimurium* food poisoning at a wedding reception. Ir J Med 92: 238-241.
2. Hosek G, Leschinsky DD, Irons S (1997) Multidrug-resistant *Salmonella* serotype Typhimurium in United States. MMWR Morb Mortal Wkly Report 46: 308-310.
3. Threlfall EJ, Frost JA, Ward LR (1996) Increasing spectrum of resistance in multiresistant *Salmonella Typhimurium*. Lancet 347: 1053-1054.
4. Threlfall EJ, Ward LR, Skinner JA (1997) Increase in multiple antibiotic resistance in non-typhoidal salmonellas from humans in England and Wales: a comparison of data for 1994 and 1996. Microb Drug Resist 3: 263-266.
5. Davies A, O'Neill P, Towers L, Cooke M (1996) An outbreak of *Salmonella typhimurium* DT104 food poisoning associated with eating beef. Commun Dis Rep CDR Rev 6: 159-162.
6. Cody SH, Abbott SL, Marfin AA (1999) Two outbreaks of multidrug-resistant Salmonella serotype Typhimurium DT104 infections linked to raw-milk cheese in Northern California. JAMA 281: 1805-1810.
7. Molbak K, Baggesen DL, Aarestrup FM (1999) An outbreak of multidrug-resistant, quinolone-resistant *Salmonella enterica* serotype Typhimurium DT104. N Engl J Med 341: 1420-1425.
8. Villar RG, Macek MD, Simons S (1999) Investigation of multidrug resistant *Salmonella* serotype Typhimurium DT104 infection inked to raw milk cheese in Washington State. JAMA 281:1811-1816.
9. Baucheron SH, Imberechts E, Chaslus-Danclaand A (2002) The AcrB multidrug transporter plays a major role in high-level fluoroquinolone resistance in *Salmonella enterica* serovar Typhimurium phage type DT204. Microb Drug Resist 8: 281-289.
10. Baucheron SE, Chaslus-Danclaand A, Cloeckaert (2004) A Role of TolC and parC mutation in high-level fluoroquinolone resistance in *Salmonella enterica* serotype Typhimurium DT204. J Antimicrob Chemother 53: 657-659.
11. Nishino K, Latifi T, Groisman EA (2006) Virulence and drug resistance roles of multidrug efflux systems of *Salmonella enterica* serovar Typhimurium. Mol Microbiol 59: 126-141.
12. Lacroix FJ, Cloeckaert A, Grepinet O (1996) *Salmonella typhimurium* acrB-like gene: identification and role in resistance to biliary salts and detergents and in murine infection. FEMS Microbiol Lett 135: 161-167.
13. Piddock LJ (2002) Fluoroquinolone resistance in *Salmonella* serovars isolated from humans and food animals. FEMS Microbiol Rev 26: 3-16.
14. Hernandez-Mendoza A, Quinto C, Segovia L (2007) Ligand-binding prediction in the resistance-nodulation-cell division (RND) proteins. Comput Biol Chem 31: 115-123.
15. Pages JM, Masi M, Barbe J (2005) Inhibitors of efflux pumps in Gram-negative bacteria. Trends Mol Med 11: 382-389.
16. Geourjon C, Deleage G (1995) SOPMA: significant improvements in protein secondary structure prediction by consensus prediction from multiple alignments. Comput Appl Biosci 11: 681-684.
17. Garnier J, Gibratand JF, Robson B (1996) GOR method for predicting protein secondary structure from amino acid sequence. Methods Enzymol 266: 540-553.
18. Sonnhammer EL, Von Heijne G, Krogh A (1998) A Hidden Markov model for predicting transmembrane helices in protein sequences. Proc Int Conf Intell Syst Mol Biol 6: 175-82.
19. Hofmann K, Stoffel W (1993) TMBASE a database of membrane spanning protein segments. Biol Chem Hoppe-Seyler 374: 166-170.
20. Hirokawa T, Boon-Chieng S, Mitaku S (1998) SOSUI: classification and secondary structure prediction system for membrane proteins. Bioinformatics 14: 378-379.
21. Tusnady GE, Simon I (2001) The HMMTOP transmembrane topology prediction server. Bioinformatics 17: 849-850.
22. Thompson JD, Higgins DG, Gibson TJ (1994) CLUSTAL W: improving the sensitivity of progressive multiple sequence alignment through sequence weighting, position-specific gap penalties and weight matrix choice. Nucleic Acids Res 22: 4673-4680.
23. Sali A, Blundell TL (1993) Comparative protein modelling by satisfaction of spatial restraints. J Mol Biol 234: 779-815.
24. Fiser A, Sali A (2003) ModLoop: Automated modeling of loops in protein structures. Bioinformatics 19: 2500-2501.
25. Laskoswki RA, MacArthur MW, Moss DS (1993) PROCHECK: A program to check the stereo chemical quality of protein structures. J Appl Cryst 26: 283-291.
26. Eisenberg D, Luthyand R, Bowie JU (1997) VERIFY3D: assessment of protein models with three-dimensional profiles. Methods Enzymol 277: 396-404.
27. Colovos C, Yeates TO (1993) Verification of protein structures: patterns of non-bonded atomic interactions. Protein Sci 2: 1511-1519.
28. Hooft RW, Vriend G, Sander C (1996) Errors in protein structures. Nature 381: 272.
29. Guex N, Peitsh MC (1997) SWISS-MODEL and the Swiss-PdbViewer: an environment for comparative protein modeling. Electrophoresis 18: 2714-2723.
30. Trott O, Olson AJ (2010) AutoDock Vina: improving the speed and accuracy of docking with a new scoring function, efficient optimization, and multithreading. J Comput Chem 31: 455-461.
31. WolfL K. PyRx. C&EN. 2009, 87:31.
32. DeLano WL (2012)The PyMOL Molecular Graphics System DeLano Scientific, San Carlos, CA, USA.